CORRECTED 28 NOVEMBER 2018; SEE ERRATUM

MUSCULAR DYSTROPHY

Anchor peptide captures, targets, and loads exosomes of diverse origins for diagnostics and therapy

Xianjun Gao[1]*, Ning Ran[1]*, Xue Dong[1], Bingfeng Zuo[1], Rong Yang[2], Qibing Zhou[2], Hong M. Moulton[3], Yiqi Seow[4], HaiFang Yin[1†]

Exosomes are circulating nanovesicular carriers of macromolecules, increasingly used for diagnostics and therapeutics. The ability to load and target patient-derived exosomes without altering exosomal surfaces is key to unlocking their therapeutic potential. We demonstrate that a peptide (CP05) identified by phage display enables targeting, cargo loading, and capture of exosomes from diverse origins, including patient-derived exosomes, through binding to CD63—an exosomal surface protein. Systemic administration of exosomes loaded with CP05-modified, dystrophin splice–correcting phosphorodiamidate morpholino oligomer (EXO_{PMO}) increased dystrophin protein 18-fold in quadriceps of dystrophin-deficient mdx mice compared to CP05-PMO. Loading CP05-muscle–targeting peptide on EXO_{PMO} further increased dystrophin expression in muscle with functional improvement without any detectable toxicity. Our study demonstrates that an exosomal anchor peptide enables direct, effective functionalization and capture of exosomes, thus providing a tool for exosome engineering, probing gene function in vivo, and targeted therapeutic drug delivery.

INTRODUCTION

Exosomes are nanoscale vesicles with sizes of 30 to 150 nm (in diameter) that are secreted by most mammalian cells and thus bear many macromolecules from their parental cells (*1*, *2*). These unique features enable exosomes to be used as diagnostic markers for pregnancy and various malignancies (*3*, *4*) and also harnessed as delivery vehicles for a large variety of cargoes ranging from anticancer chemotherapeutics to nucleic acids (*5*–*8*). To avoid triggering an immune response, therapeutic exosomes should ideally be patient-derived, and subsequent modifications should not substantially affect the structure or surface of exosomes. Current methods of targeting exosomes with therapeutic macromolecules typically involve genetic manipulation of their producer cells or chemical conjugation of peptides to exosomal surface (*9*). Genetic engineering of parental cells is labor-intensive with variable efficacy, depending on the transfection efficiency and cell types, and precludes the use of a patient's circulating exosomes for therapeutic use, whereas chemical functionalization of native exosomes, such as with click chemistry (*9*), can largely alter surface structure. Transferrin had been used to paint patient-derived exosomes with paramagnetic particles (*10*), but transferrin binds weakly to exosomes and is promiscuous because transferrin-binding molecules are abundant in blood. Electroporation (*7*), lyophilization, or transfection of parental cells (*11*, *12*) can load exosomes with macromolecules, but these methods suffer from low loading efficiencies (*13*).

To overcome these limitations, we used phage display to identify peptides that can anchor cargo and targeting moieties to exosomes. These peptides will greatly simplify the process of loading and functionalizing exosomes. Because genetic modification of producer cells is not required, patient-derived exosomes can be used.

CD63 is a tetraspanin enriched on the surface of exosomes and regarded as an exosomal marker (*14*). We selected for peptides that specifically bind to the second extracellular loop of CD63 and characterized three candidate peptides in CD63-expressing cells and exosomes. One peptide in particular, CP05, enabled direct painting of exosomes with different moieties irrespective of the origin of exosomes.

Efficient delivery of functional cargoes in vivo is well recognized as one of the biggest challenges in therapeutic gene delivery and in disease modeling. In particular, insufficient systemic delivery of antisense oligonucleotides (AOs) for Duchenne muscular dystrophy (DMD) exon-skipping therapy hinders translation to the clinic (*15*). Here, we painted exosomes, recovered by high-speed ultracentrifugation and 0.22-μm diafiltration, with a phosphorodiamidate morpholino oligomer (PMO) (*16*), currently approved by the U.S. Food and Drug Administration for treating DMD, as a CP05 conjugate, and demonstrated an 18-fold increase of dystrophin expression in quadriceps compared to naked PMO or the CP05-PMO conjugate without exosomes. CP05 also allows for simultaneous functionalization of exosomes with different moieties, including targeted PMO delivery to muscle in mdx mice by anchoring a muscle-targeting peptide and PMO on the same exosome with CP05. CP05 can anchor moieties not only to culture-derived exosomes from different cells but also to circulating exosomes from human serum. Furthermore, immobilized CP05 can also specifically capture exosomes from patients' serum. This study demonstrates that a CD63-specific exosomal anchor peptide enables direct and effective modification, cargo loading, and capture of exosomes and thus opens a new avenue for exosome engineering.

RESULTS

CP05 paints exosomes specifically through CD63

We performed in vitro selection with purified CD63 second extracellular loop (Fig. 1A) (*14*). To avoid propagation-related artifacts, only two rounds of biopanning were performed, with evident increases in recovered phage over rounds (fig. S1). The three most abundant peptides from round 2 that were identified by high-throughput

[1]Department of Cell Biology and Key Laboratory of Immune Microenvironment and Disease (Ministry of Education), Tianjin Medical University, Qixiangtai Road, Heping District, Tianjin 300070, China. [2]Department of Nanomedicine and Biopharmaceuticals, College of Life Science and Technology, Huazhong University of Science and Technology, Wuhan 430074, China. [3]Biomedical Sciences, College of Veterinary Medicine, Oregon State University, Corvallis, OR 97331, USA. [4]Molecular Engineering Laboratory, Biomedical Sciences Institutes, Agency for Science Technology and Research, 61 Biopolis Way, Singapore 138668, Singapore.
*These authors contributed equally to this work.
†Corresponding author. Email: haifangyin@tmu.edu.cn

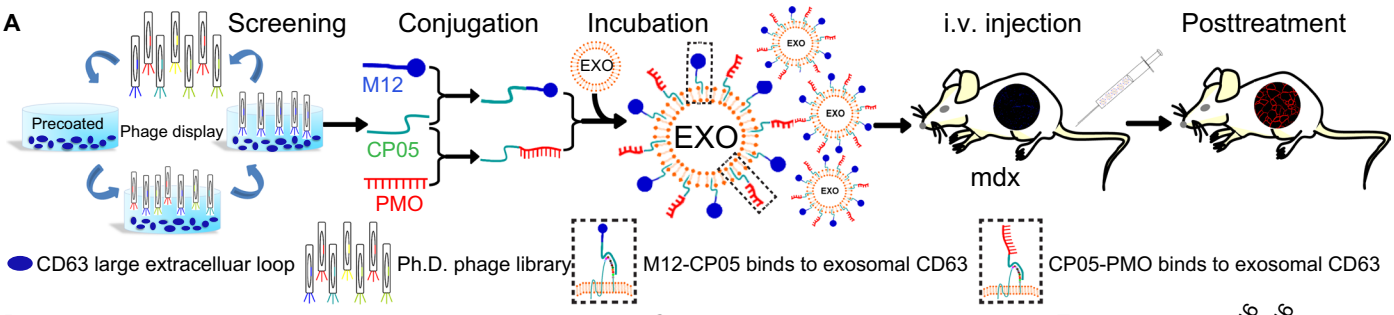

B

No.	Displayed peptide	Reads	Name
1	CRHSQMTVTSRL	15,780	CP05
2	DWSSWVYRDPQT	14,310	CP06
3	SHCLARQTMLQV	9,570	CP07
4	DRWVARDPASIF	7,550	—
5	SQDIRTWNGTRS	2,719	—
6	VEPPNSQHSGPC	2,467	—
7	VHWDFRQWWQPS	2,437	—
8	AYYPFVKGRPLP	1,435	—
9	MHPNAGHGSLMR	1,428	—
10	ASSRRPSVGKGF	1,379	—
11	VTTMSGEISQAR	962	—
12	GFPTRFEALSSN	828	—
13	TGSNSPMWDTEV	722	—
14	HVRLTGWQPTWA	306	—
15	QFDYMRPANDTH	298	—
16	SPCTSFPRCVEL	293	—
17	QLATLHKLSGPT	278	—

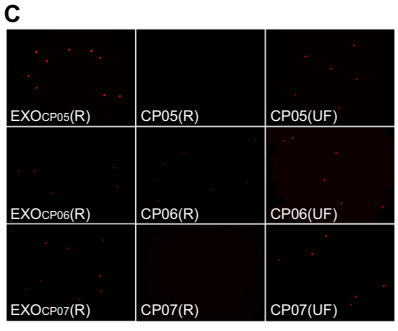

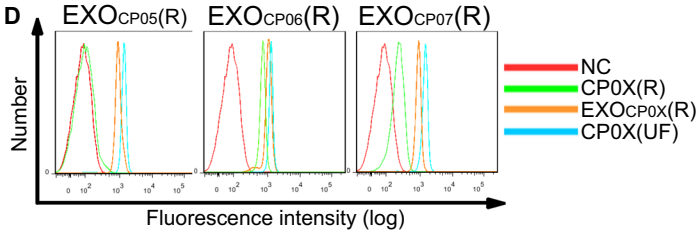

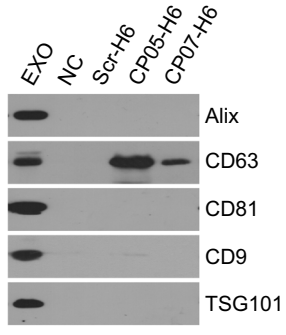

Fig. 1. CP05 binds to exosomes through CD63. (**A**) Schematic illustration of screening for exosomal anchor peptides and functionalization on exosomes. Precoated refers to CD63 large extracellular loop protein fragments coated plates. M12 means muscle-targeting peptide; PMO represents AO drugs. i.v., intravenous. (**B**) Table of the top 17 candidate peptide sequences in the order of reads by high-throughput sequencing. (**C**) Representative fluorescence microscopic images showing the binding of rhodamine-labeled candidate peptides to murine myotube-derived exosomes. $EXO_{CP0X}(R)$ refers to the bead-bound filtrated peptide-exosome complex retentates. CP0X(R) refers to the bead-bound filtrated rhodamine-labeled peptide retentates and was used as a negative control. CP0X(UF) represents the bead-bound unfiltrated rhodamina-labeled peptide and was used as a positive control. (**D**) Flow cytometry for bead-bound rhodamine-labeled peptide-exosome complexes ($n = 6$). NC refers to beads alone. CP0X represents different peptides. (**E**) Western blot results for examining the specific binding affinity of candidate peptides to murine myotube-derived exosomes via CD63. EXO refers to exosomes; Scr-H6 refers to His-tagged scrambled CP05 peptide. All exosome lysates captured by His-tagged peptides were loaded for protein assay.

sequencing were selected (Fig. 1B). Other than a polystyrene binding WSSW motif for CP06 (*17*), no known motif was identified upon alignment with PepBank (*18*), SAROTUP (*19*), and PubMed with BLAST.

Murine myotube C2C12 exosomes, characterized by expression of exosomal markers CD63, CD9, and Alix (fig. S2A) (*14*, *20*), a saucer-cup shape under transmission electron microscopy (TEM) (fig. S2B), and a buoyant density of 1.10 to 1.21 g/ml measured with sucrose gradient ultracentrifugation (fig. S2C), were incubated with rhodamine-labeled peptides. Unbound peptides were removed with serial diafiltration, and the retentates (R) were incubated with polystyrene beads for microscopy and flow cytometry. Rhodamine-labeled peptide-exosome complexes consistently had brighter fluorescence signals than rhodamine-labeled peptides alone after filtration (Fig. 1C), indicating that all three peptides interacted with exosomes. However, CP06 and CP07 retentates also fluoresced after filtration (Fig. 1C), suggesting spontaneous flocculation and interaction with beads. Flow cytometry analysis was also consistent, with stronger signals seen with peptide-exosome complexes (Fig. 1D). To ascertain whether CP05 and CP07 are specific for CD63 on exosomes, exosomes were incubated with His-tagged CP05-coated, a scrambled CP05-coated (table S1), or CP07-coated beads and lysed with protein lysis buffer. Proteins not directly bound to the beads were then washed off, and bound proteins were analyzed with Western blot. A stronger CD63 band was produced in the CP05 sample than CP07 (Fig. 1E), suggesting that CP05 specifically binds CD63 with stronger affinity than CP07, whereas nothing bound to the scrambled CP05. Strikingly, there was no specific interaction with other tetraspanins such as CD81 and CD9 or other exosomal markers including Alix and Tsg101 detected for either CP05 or CP07. A similar experiment using CD63-expressing C2C12 cell lysates verified that CP05 specifically interacts with CD63 (fig. S2D). These findings support the conclusion that CP05 binds to exosomes through CD63 specifically.

CP05 does not alter characteristics and in vivo distribution of exosomes

Morphology and size distribution of exosomes were largely unchanged upon CP05 modification (Fig. 2, A and B). To assess the modification

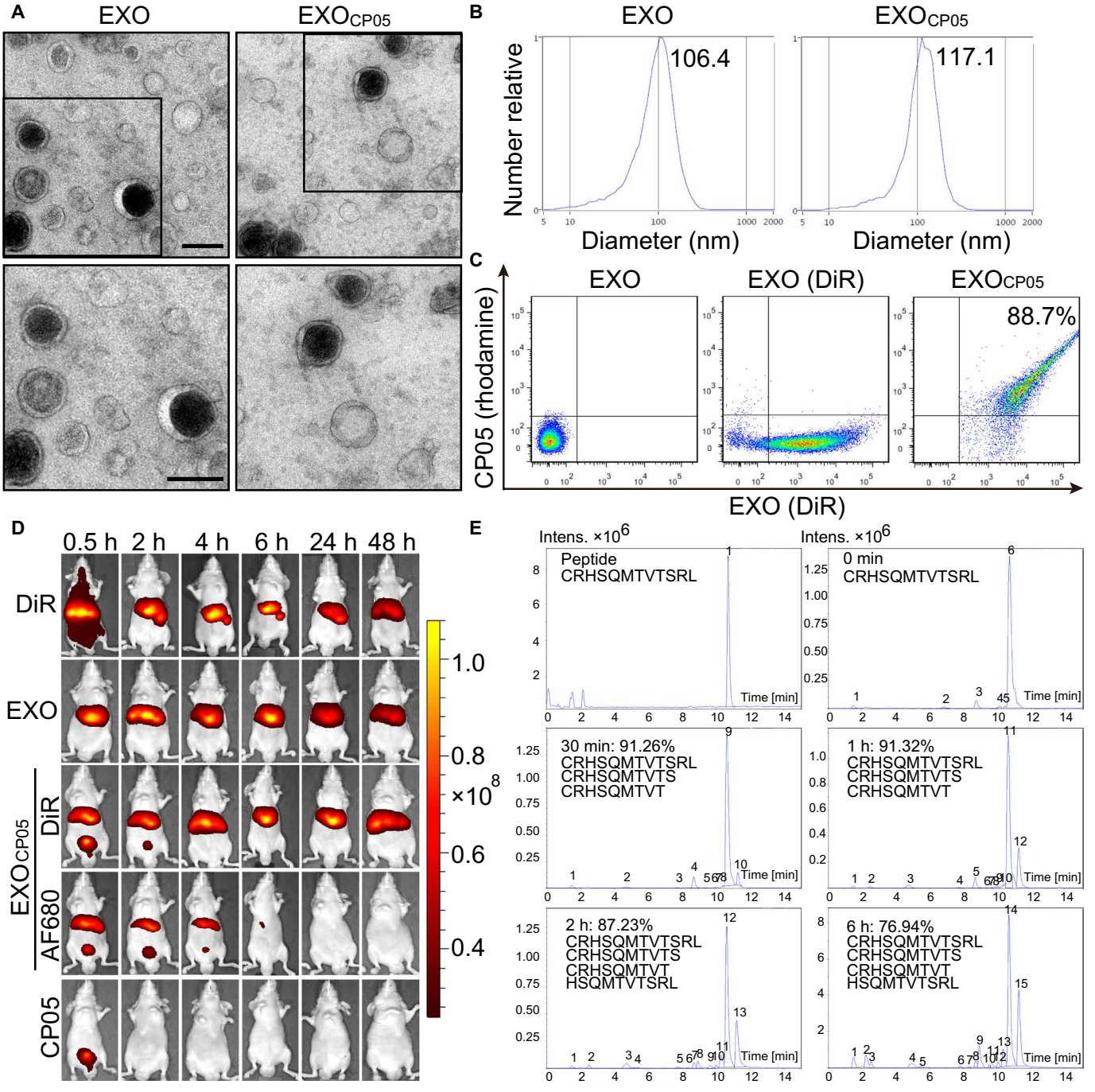

Fig. 2. Characterization of CP05-painted exosomes (EXO_{CP05}) and serum stability of CP05. (**A**) Representative TEM images for EXO and EXO_{CP05}. EXO refers to unmodified exosomes; EXO_{CP05} represents CP05-painted exosomes (scale bars, 100 nm). Bottom panels represent the corresponding magnified boxed areas from top panels. (**B**) Size distribution of EXO and EXO_{CP05}. (**C**) Flow cytometry for measuring the modification efficiency of CP05 on exosomes. Rhodamine-labeled CP05 (20 μg) and DiR-labeled (5 μg) exosomes were used. (**D**) Live animal imaging to examine the biodistribution of DiR-labeled EXO and EXO_{CP05} in wild-type C57BL/6 mice. Animals were imaged with IVIS spectrum at different time points after a single intravenous injection of 30 μg of DiR-labeled EXO_{CP05} and EXO. DiR (0.3 μg) and AF680-labeled CP05 (10 μg) were used as controls. (**E**) Measurement of serum stability of CP05 with LC-MS. Peptide or peptide fragments were assayed at different time points including 0, 30, 60, 120, and 360 min after incubation with 20% serum at 37°C.

efficiency, the percentage of exosomes painted with at least one copy of CP05, we first examined whether flow cytometry can distinguish single exosome in the absence of beads (*21*). A complete gate strategy for flow cytometry assay was established with beads of different sizes or buffers as positive or negative controls (fig. S3A). Pkh67 (green)– or DiR (red)–labeled exosomes were also evaluated with flow cytometry individually or together. Two distinct populations with no overlap would be expected if most droplets contained at most

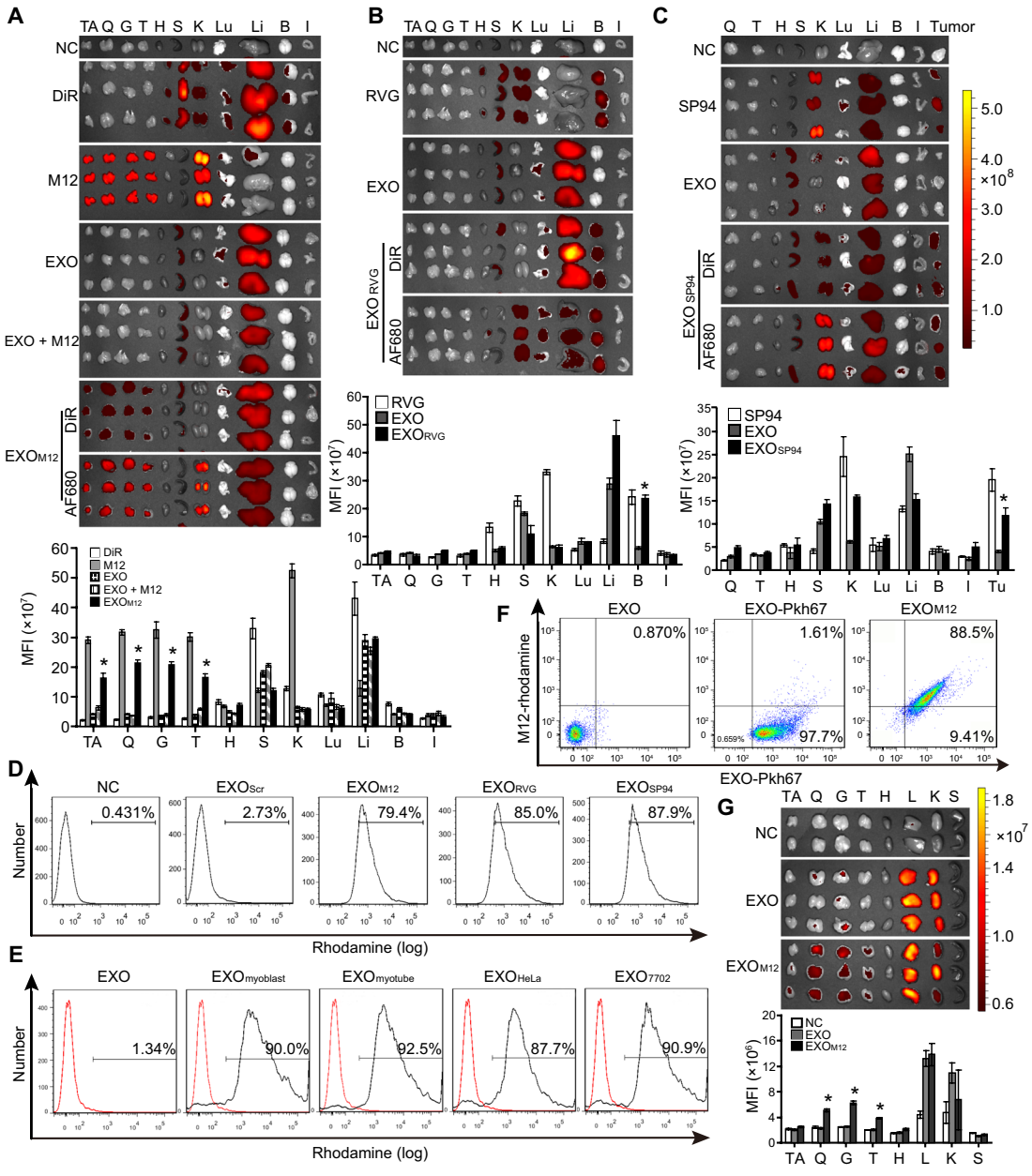

Fig. 3. Redistribution of homing moiety–painted exosomes in vivo and quantitative analysis of modification efficiency on exosomes. For in vivo distribution, AF680-labeled peptides and DiR-labeled exosomes were used, unless otherwise specified. For flow cytometry, rhodamine-labeled peptides were used, unless otherwise specified. (**A**) Tissue distribution and quantitative analysis of fluorescence intensity in body-wide muscles from C57BL/6 mice after a single intravenous injection of 30 μg of EXO, EXO + M12, and M12-CP05–painted exosomes (EXO_{M12}): EXO_{M12} versus M12 + EXO in tibialis anterior, quadriceps, gastrocnemius, and triceps (*P < 0.001). Exosomes were derived from murine myotubes. NC represents untreated control. TA, tibialis anterior; Q, quadriceps; G, gastrocnemius; T, triceps; H, heart; S, spleen; K, kidney; Lu, lung; Li, liver; B, brain; I, intestine; MFI, mean fluorescence intensity. DiR means DiR dye alone. M12 + EXO refers to the mixture of exosomes (EXO) and M12 peptides. (**B**) Tissue distribution and quantitative analysis of fluorescence intensity in brain tissue from C57BL/6 mice after a single intravenous injection of 30 μg of EXO, EXO + RVG, and RVG-CP05–painted exosomes (EXO_{RVG}): EXO_{RVG} versus RVG + EXO in the brain tissue (*P = 0.0044). RVG + EXO refers to the mixture of exosomes (EXO) and RVG peptides. Exosomes were derived from murine myotubes. (**C**) Tissue distribution and quantitative analysis of fluorescence intensity in subcutaneous HCC tumors from tumor-bearing C57BL/6 mice after a single intravenous injection of 30 μg of EXO, EXO + SP94, and SP94-CP05–painted exosomes (EXO_{SP94}): EXO_{SP94} versus SP94 + EXO in the tumor tissue (*P = 0.0191). Tu, tumor. Exosomes were derived from Hepa1-6 cells. SP94 + EXO refer to the mixture of exosomes (EXO) and SP94 peptides. (**D**) Flow cytometry to assess the modification efficiency of different homing moiety–CP05 peptides on exosomes. The percentage refers to double-positive exosomes out of DiR-positive exosome populations. (**E**) Flow cytometry to assess CP05 modification efficiency on exosomes derived from human cells. $EXO_{myoblast}$, $EXO_{myotube}$, EXO_{HeLa}, or EXO_{7702} refers to CP05-bound exosomes derived from human myoblasts, myotubes, HeLa cells, or liver cells (7702), respectively. The percentage means rhodamine-positive events out of total events. (**F**) Flow cytometry to assess CP05 modification efficiency on exosomes derived from human serum. Pkh67-labeled exosomes were used. (**G**) Tissue distribution and quantitative analysis of fluorescence intensity in peripheral muscles from immunodeficient nude mice after a single intravenous injection of 30 μg of EXO and M12-CP05–painted exosomes (EXO_{M12}): EXO_{M12} versus EXO in quadriceps (*P = 0.0049), gastrocnemius (*P = 0.0024), and triceps (*P = 0.0135). Exosome were derived from human serum. Pkh67-labeled exosomes were used. Significance was determined by two-tailed t test (n = 3). The data for the NC and EXO conditions shown in (A) are repeated in (B). Experimental groups shown in (A) and (B) were tested as part of the same experiment.

one exosome; conversely, if multiple exosomes were found per drop, then this would likely register as a double positive. Two separate populations were observed when Pkh67- and DiR-labeled exosomes were mixed (fig. S3B), demonstrating that flow cytometry can be used to characterize individual exosomes. About 88.7% of DiR-labeled exosomes were modified with rhodamine-labeled CP05, as demonstrated by flow cytometry (Fig. 2C), which is consistent with the abundance of CD63 expression on DiR-labeled exosomes (fig. S3C). Tissue distribution of DiR-labeled exosomes after intravenous administration in C57BL/6 mice was largely unaltered by CP05 modification when visualized with a small-animal imaging system (IVIS) in a real-time manner. Exosomes and EXO_{CP05} (CP05-modified exosomes)

were mainly present in the liver at different time points, and no evident redistribution was found up to 48 hours after injection (Fig. 2D). CP05 anchored on exosomes was still detectable at 4 hours after injection, whereas Alexa Fluor 680 (AF680)–labeled CP05 alone had disappeared by 2 hours after injection, indicating the ability of exosomes to protect CP05 from degradation. CP05 was incubated in 20% serum, and peptide integrity was measured at different time points with liquid chromatography–mass spectrometry (LC-MS) to establish serum stability. About 77% of the peptide remained intact after 6 hours, although trace degradation appeared after 30 min (Fig. 2E). These findings demonstrate that CP05 modification does not alter the morphology, size, and tissue distribution of exosomes, and CP05 is relatively stable in blood after systemic administration.

Painting targeting moieties via CP05 redistributes exosomes in vivo

AF680-labeled M12-CP05 conjugate, in which M12 is a muscle-targeting peptide (*22*), was incubated with DiR-labeled exosomes (EXO_{M12}) for 2 hours and intravenously injected into C57BL/6 mice. Tissues were imaged with IVIS 2 hours after injection, and significant increases in fluorescence intensity were detected in peripheral muscles from mice injected with EXO_{M12} compared to a M12 peptide–exosome mixture or exosomes alone (Fig. 3A), suggesting that M12-CP05 targets exosomes to muscle. The size and structure of EXO_{M12} were unaltered (fig. S4, A and B). Neuron-specific rabies viral glycoprotein (RVG) (*7*) peptide–CP05–painted exosomes (EXO_{RVG}) similarly redirected C2C12 exosomes to the brain in vivo under identical conditions (Fig. 3B); hepatocellular carcinoma (HCC)–targeting peptide (SP94)–CP05–painted exosomes (EXO_{SP94}) (*23*) likewise redirected CD63-expressing Hepa1-6 exosomes (fig. S4C) to the tumor in a subcutaneous HCC model (Fig. 3C). These results demonstrate that CP05 can anchor targeting peptides on exosomes and redirect systemic distribution of exosomes to specific tissues. To assess whether the modification efficiency varies with different CP05-tagged targeting moieties, we incubated rhodamine-labeled peptides with DiR-labeled exosomes and quantitatively analyzed EXO_{M12}, EXO_{RVG}, and EXO_{SP94} after filtration to remove unbound peptides. All three samples had similar modification efficiency (percentage of double-positive out of DiR-labeled exosomes), with SP94 being the highest (87.9%) (Fig. 3D). Flow cytometry analysis of rhodamine-labeled CP05 incubated with exosomes from human myoblasts, myotubes, cervical cancer (HeLa) cells, and liver cells (7702), all of which expressed CD63 (fig. S4D), revealed that CP05 can effectively bind human exosomes (Fig. 3E). Exosomes purified from human serum, which expressed exosomal markers with a saucer-cup shape (fig. S4, E and F), can be painted with M12-CP05. M12-CP05–modified serum exosomes showed about 88% of modification efficiency (Fig. 3F) and can be targeted to muscle in immunodeficient nude mice (Fig. 3G). These findings demonstrate that CP05 is capable of painting CD63-positive exosomes efficiently at the peptide/exosome ratios attempted irrespective of origins of the exosomes.

CP05 can isolate exosomes from human serum

Because CP05 showed a strong and specific binding affinity to exosomes through CD63, we next investigated whether CP05 can be used to capture exosomes from human serum. An appreciable amount of circulating exosomes was captured from human serum with His-tagged CP05 on nickel Dynabeads (108.98 ± 7.82 μg per milliliter of serum), which is about 54% of the amount captured via ultracentrifugation (200 μg/ml of serum), indicated by the expression of exosomal marker protein (Fig. 4A). Exosomes captured with CP05 showed the same typical sauce-cup shape and were within the same size range as those isolated from ultracentrifugation (Fig. 4, B and C). To assess the utility of exosomes captured through CP05, we isolated exosomes from serum from patients with HCC and pancreatic cancer and examined the expression of tumor-associated antigens such as α-fetoprotein (AFP; HCC-specific antigen) (*24*) and glypican-1 (GPC1; pancreatic cancer–specific antigen) (*25*). Abundant AFP or GPC1 protein was detected in exosomes captured via CP05 from HCC or pancreatic

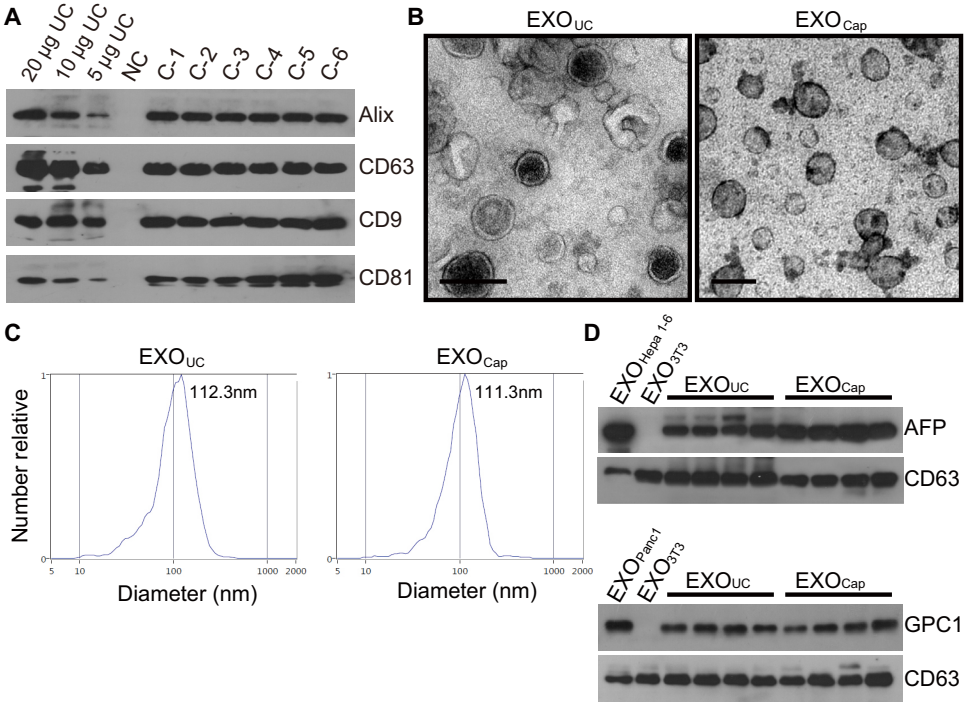

Fig. 4. Isolation of exosomes from human serum via CP05. (**A**) Western blot to show the expression of exosomal biomarkers on exosomes captured via CP05 from human serum. Exosomes isolated with ultracentrifugation (UC) were used as loading controls. NC (negative control) refers to uncoated beads mixed with human serum; C-1 to C-6 (Captured) represent exosomes captured from 1 ml of human serum with CP05-coated nickel Dynabeads after removing cell debris with centrifugation (the number indicates sample number). Exosomes (10 μg) captured with CP05 were loaded. (**B**) Representative TEM images for captured exosomes via CP05. EXO_{UC} or EXO_{Cap} refers to exosomes isolated with ultracentrifugation or captured via CP05 (scale bars, 100 nm). (**C**) Size distribution of EXO_{UC} and EXO_{Cap}. (**D**) Western blot to show the expression of tumor-specific antigens from HCC or pancreatic cancer patients' serum. $EXO_{Hepa1\text{-}6}$, EXO_{3T3}, or EXO_{Panc1} refers to exosomes isolated via ultracentrifugation from murine HCC cells, fibroblasts (negative control), or pancreatic cancer cells. Exosomes (10 μg) were loaded.

cancer patients' serum (Fig. 4D), indicating the ability of CP05 to isolate exosomes effectively.

CP05 allows dual modification of exosomes

Given the abundance of CD63 on exosomes (*26*), more than one moiety could possibly be anchored on exosomes. Rhodamine-labeled M12-CP05 and fluorescein isothiocyanate (FITC)–labeled NP41-CP05, a nerve-specific peptide (*27*), were incubated with exosomes individually or together for 2 hours and followed by diafiltration to remove unbound peptides. Unsurprisingly, most exosomes were simultaneously labeled with both peptides (Fig. 5A), suggesting that CP05 can anchor two different moieties on exosomes. We performed fluorescence resonance energy transfer (FRET) assay to ascertain the proximity of peptides present on the same exosome. As expected, stronger FRET signals were detected in exosomes modified with NP41-CP05 and RVG-CP05 than when single-labeled EXO_{NP41} and EXO_{RVG} were mixed (Fig. 5B), demonstrating that CP05 can modify individual exosomes with different moieties and the interaction is stable because the peptides are not jumping between EXO_{NP41} and EXO_{RVG}.

CP05 directs efficient PMO loading on exosomes

We wondered whether CP05 could anchor therapeutic cargoes on exosomes to enhance delivery in vivo and thus used a PMO targeting the boundary of exons 22 and 23 in murine *Dmd* gene (*16*). The morphology and size of CP05-PMO-exosome complexes (EXO_{PMO}) was unaltered (fig. S5, A and B), with a binding efficiency of 82.5% (fig. S5C). Local intramuscular injection of EXO_{PMO} into tibialis anterior muscles of mdx mice resulted in a substantial number of dystrophin-positive fibers (Fig. 6A) and significantly higher dystrophin expression (Fig. 6B) ($P = 0.0019$) compared to PMO, CP05-PMO alone, or a mixture of PMO with exosomes under identical conditions, showing that CP05-mediated exosomal delivery can improve PMO uptake in muscle. Colocalization of DiR-labeled exosomes with dystrophin-positive fibers was detected in EXO_{PMO}-treated tibialis anterior muscles at 1 week after intramuscular injection of EXO_{PMO} (fig. S5D), showing the association between exosome-mediated delivery and dystrophin restoration. Systemic administration of EXO_{PMO} into adult mdx mice at 12.5 mg of PMO per kilogram per week for 3 weeks induced a substantial number of dystrophin-positive fibers in peripheral muscles compared to CP05-PMO or PMO under identical conditions, although no dystrophin was restored in the heart at this dose (Fig. 6C). Consistently, significantly higher efficiency of exon 23 skipping was detected in peripheral muscles from mdx mice treated with EXO_{PMO} compared to corresponding tissues treated with either CP05-PMO or PMO (Fig. 6D) ($P < 0.05$). The same pattern was seen with dystrophin protein expression (Fig. 6, E and F). The most marked elevation was found in quadriceps, with dystrophin expressed 18.5-fold higher than control treatments (Fig. 6F) ($P < 0.05$). Compared to single injection of EXO_{PMO} at 12.5 mg of PMO per kilogram in adult mdx mice, three weekly repeated injections of EXO_{PMO} elicited more dystrophin-positive fibers and significantly higher efficiency of exon skipping and dystrophin restoration in tibialis anterior ($P = 0.042$), quadriceps ($P = 0.032$), gastrocnemius ($P = 0.0331$),

A

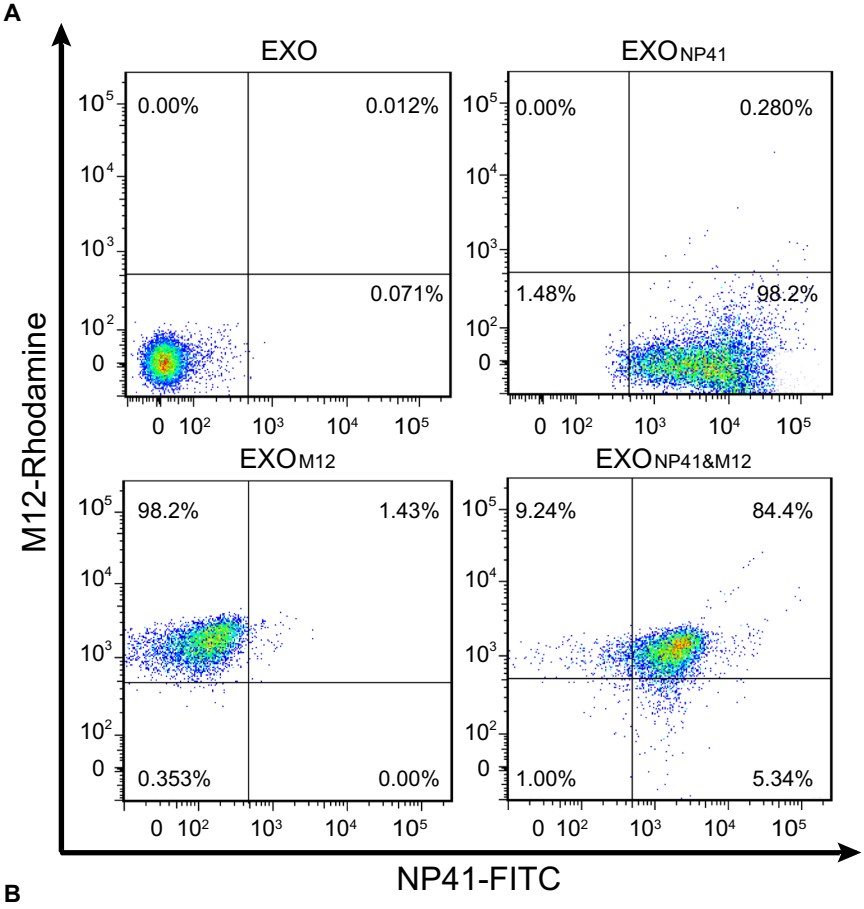

B

Group	Ex(488)/Em(520)	Ex(540)/Em(625)	Ex(488)/Em(625)
EXO_{NP41}(FITC)	2241.87 ± 125.61	4.50 ± 1.93	97.53 ± 2.03
EXO_{RVG}(RhoB)	137.37 ± 1.57	903.33 ± 102.47	425.67 ± 22.00
NP41(FITC) + RVG(RhoB)	79.80 ± 0.29	25.20 ± 2.14	29.07 ± 1.77
EXO_{NP41} (FITC) + EXO_{RVG}(RhoB)	2548.40 ± 140.20	442.00 ± 126.72	1217.33 ± 15.62
$EXO_{NP41\&RVG}$	2861.97 ± 159.08	434.77 ± 49.75	4069.00 ± 26.08

Fig. 5. Dual functionalization on exosomes with different homing moieties. (**A**) Flow cytometry to measure the dual painting efficiency of different homing moiety–CP05 peptides on exosomes. Exosomes were derived from murine myotubes. FITC-labeled NP41-CP05 and rhodamine-labeled M12-CP05 were co-incubated with exosomes individually or together. EXO_{NP41} refers to NP41-CP05–painted exosomes; EXO_{M12} refers to M12-CP05–painted exosomes. $EXO_{NP41\&M12}$ represents exosomes painted by NP41-CP05 and M12-CP05. (**B**) Table of FRET assay results for dual modification of exosomes. FRET was used to examine the simultaneous binding of different moieties on the same exosome. EXO_{RVG}(RhoB) refers to rhodamine-labeled RVG-CP05–painted exosomes. EXO_{NP41}(FITC) + EXO_{RVG}(RhoB) means the mixture of EXO_{NP41}(FITC) and EXO_{RVG}(RhoB). $EXO_{NP41\&RVG}$ represents exosomes painted by NP41-CP05 and RVG-CP05 ($n = 6$, mean ± SEM). Ex, excitation; Em, emission.

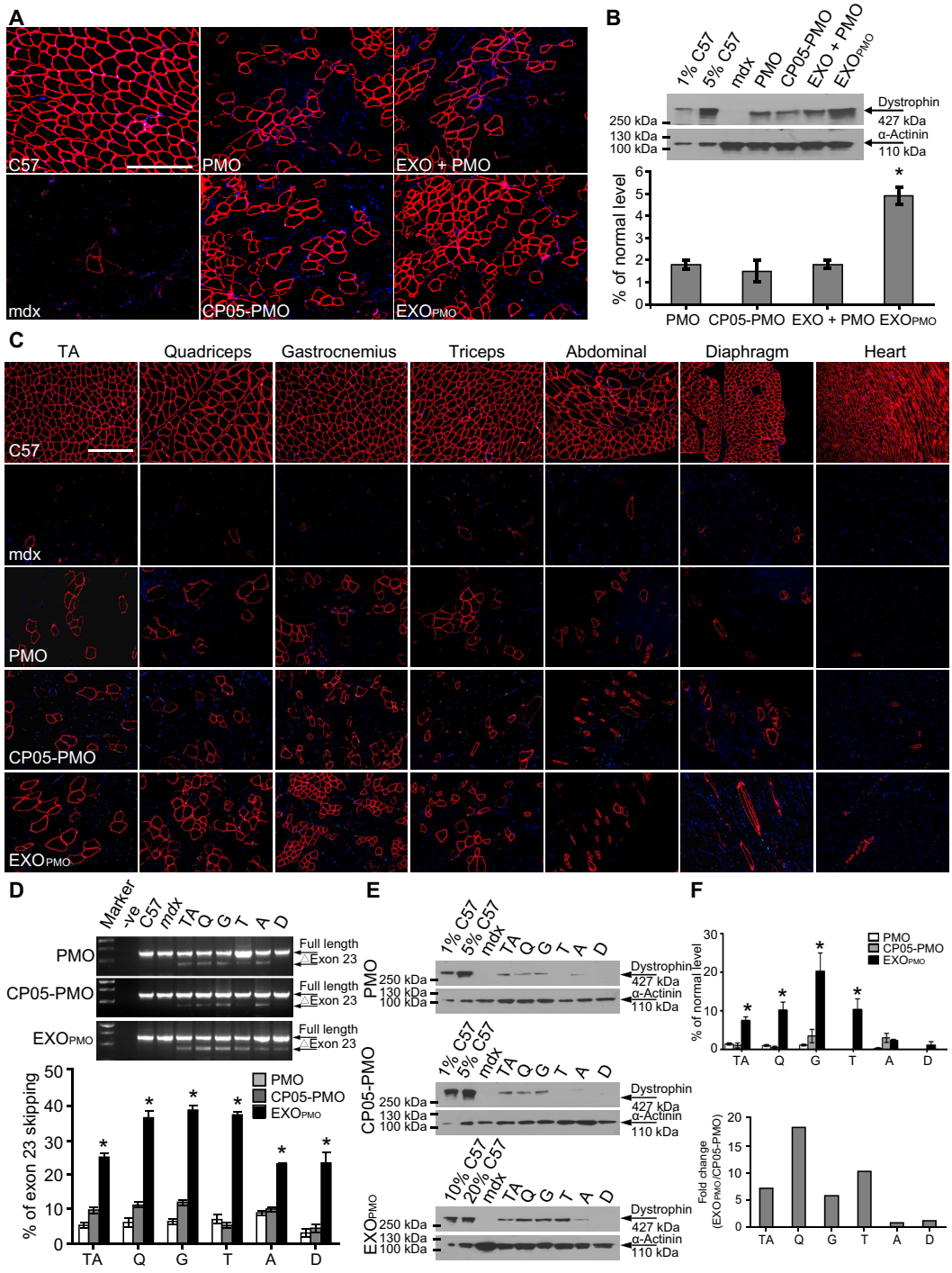

Fig. 6. Local and systemic evaluation of CP05-PMO–painted exosomes (EXO_{PMO}) in mdx mice. (**A**) Immunostaining of dystrophin-positive fibers in tibialis anterior muscle of C57BL/6 (C57) and mdx mice after intramuscular injection of 1 μg of PMO, EXO + PMO, CP05-PMO, or EXO_{PMO}. EXO + PMO refers to the mixture of exosomes with PMO. Nuclei were counterstained with 4′,6-diamidino-2-phenylindole (blue) (scale bar, 200 μm). (**B**) Western blot to measure the dystrophin restoration in tibialis anterior muscles from mdx mice treated with PMO, EXO + PMO, CP05-PMO, or EXO_{PMO}. α-Actinin was used as a loading control. The percent C57 represents 100% C57 protein extracted from tibialis anterior diluted at 1:100 and 1:20, and 5 μg of total protein from C57BL/6 and 50 μg from untreated or mdx mice treated with PMO, EXO + PMO, CP05-PMO, or EXO_{PMO} was loaded. Bar plot shows quantification of dystrophin expression of PMO-, CP05-PMO–, EXO + PMO–, or EXO_{PMO}-treated tibialis anterior normalized to untreated mdx controls. The truncated dystrophin was indistinguishable from that of normal dystrophin because there is a difference of only 71 amino acids (encoded by exon 23). (**C**) Immunostaining for dystrophin-positive fibers in body-wide muscles from mdx mice after intravenous injection of PMO, CP05-PMO, or EXO_{PMO} at the dose of 12.5 mg of PMO per kilogram per week for 3 weeks (scale bar, 200 μm). (**D**) Reverse transcription polymerase chain reaction (RT-PCR) to examine the exon skipping efficiency in body-wide muscles from mdx mice treated with PMO, CP05-PMO, or EXO_{PMO}. ΔExon 23 refers to exon 23–skipped bands. -ve means blank control. C57 and mdx refer to untreated C57BL/6 and mdx controls. A, abdominal muscle; D, diaphragm. (**E**) Western blot to examine dystrophin restoration in body-wide peripheral muscles of mdx mice treated with PMO, CP05-PMO, or EXO_{PMO}. α-Actinin was used as a loading control. One, 5, 10, and 20% C57 represents 100% C57 protein extracted from tibialis anterior that was diluted at 1:100, 1:20, 1:10, or 1:5, respectively. Total protein (50 μg) extracted from untreated and treated mdx mice was loaded. (**F**) Quantitative analysis of dystrophin restoration with ImageJ and fold change of EXO_{PMO} relative to CP05-PMO: EXO_{PMO} versus PMO and CP05-PMO in tibialis anterior (*P = 0.046), quadriceps (*P = 0.006), gastrocnemius (*P = 0.019), and triceps (*P = 0.033). Significance was determined by two-tailed t test (n = 4, mean ± SEM).

and triceps (P = 0.0396) (fig. S6). These data indicate that CP05-mediated anchoring PMO on exosomes can enhance PMO delivery in mdx mice.

CP05 enables targeted delivery of PMO to muscle

M12-CP05 and CP05-PMO were co-incubated with exosomes and injected into mdx mice intravenously at 12.5 mg of PMO per kilogram per week for 3 weeks. The combination of muscle-targeting peptide, PMO, and exosome ($EXO_{PMO\&M12}$) significantly enhanced the number of dystrophin-positive myofibers in quadriceps (P = 0.0054), gastrocnemius (P = 0.0018), and triceps (P = 0.0455) from treated mdx mice compared to EXO_{PMO} under identical conditions, although no enhancement was observed in the heart (Fig. 7A). Consistently, significantly higher efficiency of exon skipping (Fig. 7B) and expression of dystrophin (Fig. 7C) were achieved in

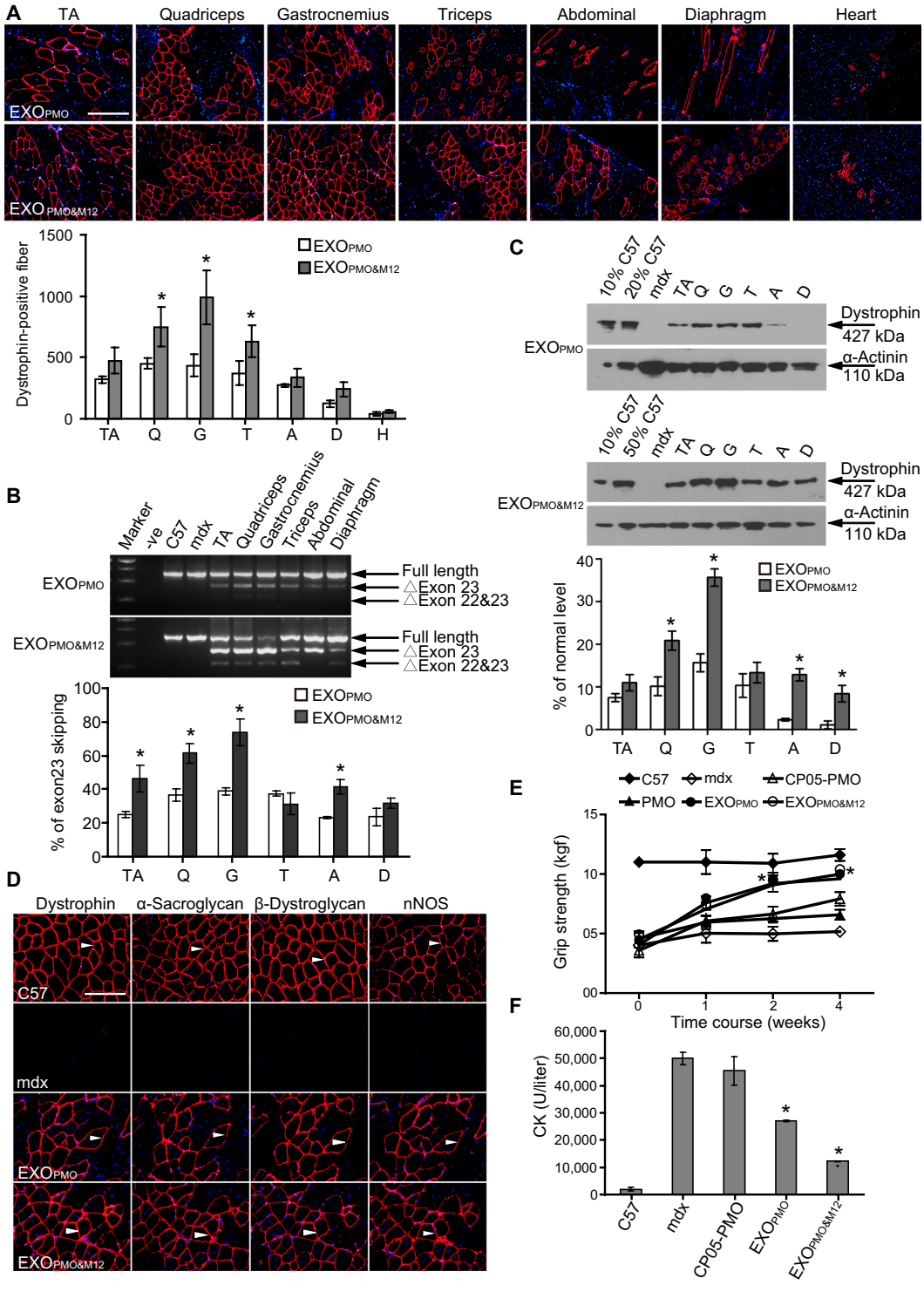

Fig. 7. Systemic evaluation of exosomes simultaneously painted by CP05-PMO and M12-CP05 ($EXO_{PMO\&M12}$) in mdx mice. Body-wide muscles were harvested and examined after intravenous injection of $EXO_{PMO\&M12}$ at the dose of 12.5 mg of PMO per kilogram per week for 3 weeks. (**A**) Immunostaining of dystrophin-positive fibers and quantification of dystrophin-positive myofibers in body-wide muscles from mdx mice treated with EXO_{PMO} and $EXO_{PMO\&M12}$: $EXO_{PMO\&M12}$ versus EXO_{PMO} in quadriceps (*P = 0.0054), gastrocnemius (*P = 0.0018), and triceps (*P = 0.0455). A, abdominal muscle; D, diaphragm (scale bar, 200 μm). (**B**) RT-PCR to determine the efficiency of exon skipping in muscles from mdx mice treated with $EXO_{PMO\&M12}$ and EXO_{PMO}: $EXO_{PMO\&M12}$ versus EXO_{PMO} in tibialis anterior (*P = 0.009), quadriceps (*P = 0.041), gastrocnemius (*P = 0.003), and abdominal muscles (*P = 0.005). ΔExon 23 or Δexon 22&23 refers to exon 23– or exons 22 and 23–skipped bands, respectively. (**C**) Western blot to determine dystrophin restoration in peripheral muscles from mdx mice treated with $EXO_{PMO\&M12}$ and EXO_{PMO}. α-Actinin was used as a loading control. Ten, 20, and 50% C57 represents 100% C57 protein extracted from tibialis anterior that was diluted at 1:10, 1:5, or 1:2, respectively. Total protein (50 μg) from muscle samples from untreated and treated *mdx* mice were loaded. Quantitative analysis of dystrophin restoration in muscle from mdx mice treated with $EXO_{PMO\&M12}$ or EXO_{PMO} (n = 6) with ImageJ is shown below: $EXO_{PMO\&M12}$ versus EXO_{PMO} in quadriceps (*P = 0.0266), gastrocnemius (*P = 0.04), abdominal muscles (*P = 0.002), and diaphragm (*P = 0.0278). (**D**) Immunofluorescence images showing relocalization of DAPC components in C57BL/6 normal controls (top panel), untreated mdx controls (second panel), mdx mice treated with EXO_{PMO} (third panel), or $EXO_{PMO\&M12}$ (bottom panel) to assess dystrophin function and recovery of normal myoarchitecture. The arrowheads point to identical myofibers in serial sections. nNOS, neuronal nitric oxide synthase (scale bar, 50 μm). (**E**) Muscle functional assessment to determine physical improvement over time in C57BL/6 normal controls, untreated mdx controls, and mdx mice treated with EXO_{PMO} or $EXO_{PMO\&M12}$. (**F**) Measurement of serum CK as an index of ongoing muscle membrane instability in C57BL/6 normal controls, untreated mdx controls, and mdx mice treated with CP05-PMO, EXO_{PMO}, or $EXO_{PMO\&M12}$: EXO_{PMO} versus CP05-PMO (*P = 0.0024), $EXO_{PMO\&M12}$ versus CP05-PMO (*P = 0.0001), and $EXO_{PMO\&M12}$ versus EXO_{PMO} (*P = 0.0083). Significance was determined by two-tailed t test (n = 4, mean ± SEM). The data for the EXO_{PMO} condition shown in Fig. 6, D and E are repeated in (B and C) and fig. S6B. Single injection of EXO_{PMO}, triple injection of EXO_{PMO}, PMO, CP05-PMO, and $EXO_{PMO\&M12}$ conditions shown in these figures were tested simultaneously as part of one experiment.

peripheral muscles treated with $EXO_{PMO\&M12}$ compared to EXO_{PMO}, indicating that CP05 enabled targeted efficient delivery of PMO to muscle.

Pathological improvement was demonstrated by relocalization of dystrophin-associated protein complex (DAPC) components (*28*), which fail to localize to the sarcolemma in the absence of dystrophin,

in $EXO_{PMO\&M12}$- and EXO_{PMO}-treated samples (Fig. 7D). Functional rescue was evident from force recovery in the grip strength test, with significant improvement in mdx mice treated with $EXO_{PMO\&M12}$ and EXO_{PMO}, compared with CP05-PMO, PMO, and mdx controls ($P = 0.0033$) (Fig. 7E), indicating that $EXO_{PMO\&M12}$ and EXO_{PMO} elicit functional rescue in mdx mice. Analysis of serum biochemical indices, including serum creatine kinase (CK) ($P < 0.005$) (Fig. 7F) (*29*), usually elevated in mdx mice; aspartate aminotransferase (AST) ($P < 0.01$) (Fig. 8A) and alanine aminotransferase (ALT) ($P < 0.05$) (Fig. 8A) showed significant decreases in mdx mice treated with $EXO_{PMO\&M12}$ and EXO_{PMO}, compared to CP05-PMO, PMO, and mdx controls, whereas there was no change in the concentrations of alkaline phosphatase (ALP) (Fig. 8A), blood urea nitrogen (BUN), and creatinine (Crea) (Fig. 8B), and histology revealed no evidence of liver or renal toxicity (Fig. 8C). Examination of inflammation revealed no alteration on inflammatory conditions in the kidney, liver, and muscle from mdx mice treated with $EXO_{PMO\&M12}$ or EXO_{PMO} compared to CP05-PMO, PMO, and mdx controls (Fig. 8, D and E), suggesting that CP05-exosome complexes do not result in any detectable toxicity. Together, these findings demonstrate that CP05 enables safe and targeted delivery of therapeutic cargo via exosomes and is a valuable tool for exosome engineering.

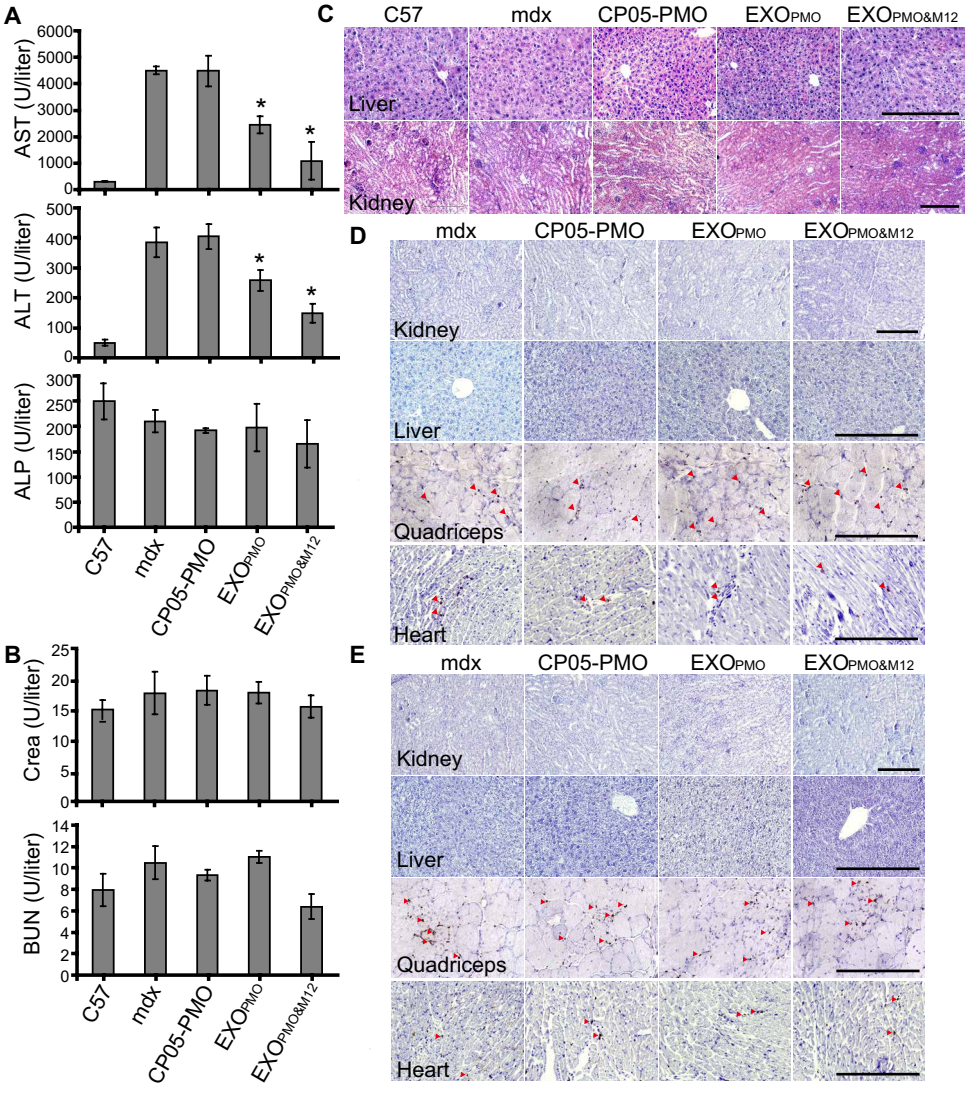

Fig. 8. Assessment of toxicity and inflammation in $EXO_{PMO\&M12}$-treated mdx mice. (**A**) Measurement of serum AST, ALT, and ALP enzymes in C57BL/6 normal controls (C57), untreated mdx controls, and mdx mice treated with CP05-PMO, EXO_{PMO}, and $EXO_{PMO\&M12}$: EXO_{PMO} versus CP05-PMO (*$P = 0.0032$), $EXO_{PMO\&M12}$ versus CP05-PMO (*$P = 0.0004$), and $EXO_{PMO\&M12}$ versus EXO_{PMO} (*$P = 0.0012$). (**B**) Measurement of serum Crea and BUN in C57BL/6 normal controls (C57), untreated mdx controls, and mdx mice treated with CP05-PMO, EXO_{PMO}, and $EXO_{PMO\&M12}$. (**C**) Hematoxylin and eosin (H&E) staining of liver (top) and kidney (bottom) tissue sections from C57BL/6 normal controls, untreated mdx controls, and mdx mice treated with CP05-PMO, EXO_{PMO}, and $EXO_{PMO\&M12}$ (scale bars, 200 μm). (**D** and **E**) Immunohistochemistry for CD3 T lymphocytes (D) and macrophages (E) in the kidney, liver, and muscle from mdx mice treated with CP05-PMO, EXO_{PMO}, $EXO_{PMO\&M12}$, and untreated mdx controls (scale bars, 100 μm). The arrowheads point to $CD3^+$ T lymphocytes or $CD68^+$ macrophages. Significance was determined by two-tailed *t* test ($n = 4$, mean ± SEM).

DISCUSSION

Here, we identified an anchor peptide specific for the second extravesicular loop of CD63. This peptide can bind to CD63-expressing exosomes irrespective of origin, including human circulatory exosomes. This peptide enables efficient modification of the same exosome with different moieties and thus allows for specific targeting of different therapeutic cargoes to desired tissues, making CP05-modified exosomes worth further exploration as safe and efficient delivery vehicles for different types of therapeutics.

CP05 also presents the possibility of capturing and using patient-derived exosomes to deliver therapeutic cargoes to target organs. Our study provides evidence that this exosomal anchor peptide can anchor various types of homing moieties, which could be used to potentially paint antigenic epitopes and immunoadjuvant molecules on exosomes. Exosomes have been considered as a natural alternative to liposomes as delivery systems because of their low/no immunogenicity, evasion from phagocytosis by monocytes and macrophages, and enhanced retention in the circulation (*25*, *30*). Patient exosomes captured from serum with CP05 could potentially be used to modify exosomes for therapeutic purposes, particularly to avoid immunological reactions that could be associated with foreign exosomes. This delivery method makes use of the natural uptake of unmodified exosomes by endogenous mechanisms (*31*) and should translate easily to clinical use. As a proof of concept, therapeutic amounts of dystrophin were achieved with EXO_{PMO} at extremely low doses of PMO and elicited functional rescue in mdx mice without any detectable toxicity, indicating that the exosome is an efficient delivery vehicle for PMO.

Beyond peptides and AOs, CP05 can theoretically be used to anchor any moiety on exosomes as long as the moiety can be conjugated to CP05. It is also likely to load other AOs on exosomes, such as 2′-*O*-methyl phosphorothioate RNA (2′OMe). Therefore, CP05 can be broadly applied to the loading of a large variety of cargoes on exosomes and thus applicable to different diseases. This study demonstrates that efficient oligonucleotide delivery can be achieved with CP05-conjugated exosomes in mice. The ability to mix and match targeting and cargo moieties with ready-made exosomes from different cellular sources gives researchers a tool to rapidly deliver macromolecules into specific tissues to answer specific biological questions. Further use could include a variety of therapeutic, targeting peptide, and oligonucleotide combinations, such as targeting neurodegenerative diseases with therapeutic PMO and neuron-specific RVG peptide conjugated via CP05 on exosomes.

This study also demonstrates that exosomes can be harvested from human serum for diagnostics using CP05, as indicated by the detection of specific cancer biomarkers from cancer patient serum. CP05 is a short peptide that would be cheaper to produce and easier to conjugate than monoclonal antibodies currently used to isolate exosomes specifically. Thus, CP05 would be an attractive prospect to develop for clinical diagnostics.

In conclusion, this study demonstrates a proof of concept for the direct, effective modification, cargo loading, and capture of exosomes via an exosomal anchor peptide, which can simplify the procedure for genetic engineering and cargo loading of exosomes. This technology should be of general utility for research and therapeutic applications in other disease models.

MATERIALS AND METHODS

Study design

Here, we designed a study to (i) identify an exosomal peptide via phage display screening, (ii) validate the binding affinity and specificity, (iii) test the modification efficiency with tissue-targeting peptides, (iv) evaluate efficiency of circulatory exosome capture, and (v) treat dystrophin-deficient mdx mice with exosomes modified with both muscle-targeting peptide and exon-skipping oligonucleotides. For functional, histological, and molecular evaluations, the number of animals per group was minimized to three to six mice, as specified in the figure legends. Numbers were determined by the investigator on the basis of previous experimental experience. All experimental procedures were carried out in the animal unit (Tianjin Medical University, Tianjin, China) according to procedures authorized by the institutional ethical committee (permit no. SYXK 2009–0001).

Cell culture

Murine C2C12 cells (mouse myoblasts) were maintained in house and cultured as previously reported (*32*). Briefly, cells were grown at 37°C in 5% CO_2 in Dulbecco's modified Eagle's medium (DMEM) supplemented with 10% fetal calf serum (FBS) and 1% penicillin and streptomycin. Mouse Hepa1-6 was purchased from Boster Biological Technology Ltd. and cultured in DMEM medium with 2 mM glutamine and 10% FBS, as per the manufacturer's instructions. Human myoblasts were provided by J. Morgan (University College London Institute of Child Health, London, UK) and were cultured in skeletal muscle cell growth medium (PromoCell) supplemented with 1.5% GlutaMAX (Gibco), 20% FBS, and 1% penicillin and streptomycin. Myotubes were obtained from confluent C2C12 or human myoblasts seeded in gelatin-coated 12-well plates after 3 days of serum deprivation at 37°C under a 5% CO_2 atmosphere in DMEM with 5% horse serum (HyClone). Primary human liver (7702) and human HeLa cells were provided by N. Zhang (Tianjin Medical University, Tianjin, China) and cultured as previously described (*33*, *34*).

Animals and injections

Six- to 8-week-old mdx (*Dmd*^{mdx}; dystrophin-deficient) and immunodeficient nude mice were purchased from the Jackson Laboratory and used in all experiments (three mice in each of the test and control groups, unless otherwise specified). C57BL/6 mice were used as wild-type controls and also for establishing subcutaneous HCC models (three mice in each of the test and control groups). Briefly, Hepa1-6 cells were digested with 0.25% trypsin in the logarithmic phase. Hepa1-6 (3×10^6) cells were suspended in 50 μl of phosphate-buffered saline (PBS) and subcutaneously injected into left axilla of C57BL/6 mice using a 1-ml syringe.

For local intramuscular injection, 1 μg of PMO, CP05-PMO, or EXO_{PMO} was dissolved in saline. For the colocalization study, 2 μg of PMO was used with DiR-labeled exosomes (2 μg) and injected into tibialis anterior muscles of adult mdx mice. For intravenous injections, various amounts of PMO, CP05-PMO, EXO_{PMO}, or $EXO_{M12\&PMO}$ in 100 μl of saline solution were injected into tail veins of mdx mice at 12.5 mg of PMO per kilogram per week (1:1 ratio for PMO and EXO) for 1 or 3 weeks. Mice were sacrificed by terminal anesthesia, followed by perfusion at desired time points, and muscles and other tissues were snap-frozen in liquid nitrogen–cooled isopentane and stored at −80°C.

Peptide, PMO, and PMO-peptide conjugates

The PMO sequence against the boundary sequences of exon and intron 23 of murine *Dmd* gene was 5′-ggccaaacctcggcttacctgaaat-3′ and designated as 25-nucleotide oligomer PMO (table S1) (*16*). PMOs were synthesized by Gene Tools LLC. Conjugations of CP05 with PMO were synthesized by a stable amide linker. All conjugates are provided by H.M.M. (Oregon State University, Corvallis, OR, USA). Fluorescence-labeled and chimeric peptides of M12-CP05, RVG-CP05, SP94-CP05, and NP41-CP05 were synthesized and provided with >95% purity by Chinapeptide Co. Ltd. Detailed AO and peptide sequences are shown in table S1.

In vitro biopanning

The Ph.D.-12 phage display library (New England BioLabs) was used for in vitro biopanning experiments. Purified CD63 protein fragment containing the second extracellular loop (LEL) (Life Technologies) was used for in vitro selection. Briefly, 20 μg of CD63 LEL purified protein was precoated onto Corning 96-well White Polystyrene Medium Bind Stripwell microplates (Corning) overnight, and unbound protein was removed and washed with PBS, followed by blocking with 5% bovine serum albumin (BSA) in PBS. Phages (1×10^{12} plaque-forming units) were incubated with CD63 LEL purified protein for 2 hours, and unbound phages were removed by washing with PBS solution for three times. The bound phages were recovered with glycine-HCl buffer (pH 2.2), followed by neutralization with tris-HCl buffer (pH 8.8). Recovered phages were titered and amplified for subsequent cycles. This process was repeated twice, and the recovered phage clones' sequences were identified by high-throughput sequencing (Genewiz).

Preparation and purification of exosomes

Cell culture medium was sequentially centrifuged at 1000*g* for 10 min, followed by 10,000*g* for 30 min. The supernatant was collected and filtered with a 0.22-μm filter (Millex), followed by ultracentrifugation at 100,000*g* for 1 hour to pellet exosomes. Exosome pellets were washed in a large volume of PBS and recovered by centrifugation at 100,000*g* for 1 hour. The total protein concentration of exosomes was quantified by the Bradford assay (Sangon Biotech). For human serum exosome isolation, human serum was obtained from healthy volunteers (provided by Tianjin Blood Center, Tianjin, China) and centrifuged at 3000*g*, 6000*g*, and 10,000*g* twice for 30 min each time to remove cell debris. The supernatant was transferred into a fresh tube, filtered with a 0.22-μm filter, and pelleted by ultracentrifugation (Beckman Optima L-100 XP, Beckman Coulter) at 100,000*g* for 1 hour and further purified by sucrose density gradient centrifugation. Exosomes were layered on a linear sucrose gradient (0.65, 0.85, 1.05, 1.25, 1.45, and 1.65 M sucrose; Sigma-Aldrich). The gradients were centrifuged for 18 hours at 100,000*g* at 4°C. Six fractions from 0.65 to 1.65 M sucrose gradients were collected and ultracentrifuged at 100,000*g* for 1 hour at 4°C to pellet exosomes. The exosome pellets were dissolved in PBS, and the total protein concentration of exosomes was quantified by the Bradford assay (Sangon Biotech).

Characterization of exosomes

Exosomal size distribution was measured by Nano Particle Tracking and Zeta potential distribution analyzer (ParticleMetrix-PMX). Morphology was visualized using a high-resolution transmission electron microscope (Hitachi HT7700). Briefly, the resuspended exosomes were diluted into water (1 μg/μl) and mixed with an equal volume of 4% paraformaldehyde. Exosomes were adsorbed onto a glow-discharged, carbon-coated formvar film attached to a metal specimen grid. Excess solution was blotted off, and the grid was immersed with a small drop (50 μl) of 1% of glutaraldehyde for 5 min, followed by washing with 100 μl of distilled water for eight times (2 min each time). Subsequently, the grid was transferred to 50 μl of uranyl-oxalate solution (pH 7.0) for 5 min and then to 50 μl of methyl cellulose-uranyl acetate (100 μl of 4% uranyl acetate and 900 μl of 2% methyl cellulose) for 10 min on ice. The excess solution was blotted off, and the sample was dried and examined in the transmission electron microscope.

Exosome capture from human serum

Human serum was obtained from healthy volunteers (n = 10), provided by Tianjin Blood Center (Tianjin, China) or HCC (n = 15) or pancreatic cancer patients (n = 18) (provided by Tianjin Medical University Cancer Institute and Hospital). All patients provided written informed consent for the sample collection. This study was conducted in accordance with Declaration of Helsinki and was approved by the Tianjin Medical University Cancer Institute and Hospital Ethics Committee. Serum was centrifuged to remove cell debris, as described above, followed by diafiltration with a 0.22-μm filter. His-tagged CP05 (200 μg/ml) was incubated with nickel Dynabeads (20 μl; Solarbio) at room temperature for 2 hours to allow CP05 to bind to beads, followed by washing with washing buffer [20 mM Na_2HPO_4, 500 mM NaCl, and 75 mM imidazole (pH 7.4)] three times to remove unbound peptides. Subsequently, recovered beads were added into the precentrifuged serum (200 μl) and incubated for 30 min at 4°C under rotation. After incubation, the supernatant was discarded, the beads were washed three times with washing buffer, and exosomes were eluted with elution buffer [20 mM Na_2HPO_4, 500 mM NaCl, and 500 mM imidazole (pH 7.4)]. Captured exosomes were used for TEM, size distribution, and Western blot analysis, as described above. Rabbit polyclonal AFP (1:1000; Abcam) and GPC1 (1:1000; Abcam) antibodies were used to examine the expression of AFP and GPC1 in captured exosomes.

Fluorescence microscopy and flow cytometry

To measure the binding affinity of candidate peptides on exosomes, exosomes (30 μg) derived from C2C12 myotubes (unless otherwise specified) were preincubated with rhodamine-labeled CP05, CP06, or CP07 peptide (30 μg) overnight at 4°C, followed by washing with PBS for five times in 2-ml ultracentrifuge tubes and filtration with 100-kDa diafiltration tube (Millipore) to remove unbound peptides. Subsequently, peptide-exosome complexes (30 μg) were incubated with 4-mm aldehyde/sulfate latex beads (Invitrogen) for 15 min at room temperature under rotation and washed with PBS for three times. Recovered beads were observed with a conventional fluorescence microscope (FV1000, Olympus) or subjected to flow cytometry (FACSCalibur, BD). Uncoated beads were used as negative controls for gating. To validate flow cytometry (FACSCalibur, BD) for direct measurement of exosomes, we first tested the following: (i) the buffer used to dissolve exosomes to evaluate the buffer background noise; (ii) the resuspended pellet from a 100,000*g* ultracentrifugation of cell culture medium to evaluate the background noise; and (iii) 100-nm and 200-nm beads (polystyrene sphere, Ruixibio) to define the target populations. Reference beads were used to set the voltages and the thresholds for measurement, as well as provide reference for gating of beads in the forward-scatter/side-scatter channels. To examine whether flow cytometry can be used to characterize individual exosomes, we labeled exosomes with Pkh67 (Sigma-Aldrich) or DiR (Life Technologies) as per the manufacturer's instruction and subjected to flow cytometry individually or together. To measure the percentage of CD63-positive exosomes in total exosomes, DiR-labeled exosomes (5 μg) were incubated with phycoerythrin (PE)–Cy7–labeled anti-mouse CD63 antibody (1:20; eBioscience) or PE-Cy7–labeled rat immunoglobulin G2a (IgG2a) isotype control (1:20; eBioscience) in 4% BSA for 30 min at 4°C, followed by 1:10 dilution with PBS, and were analyzed with flow cytometry (FACSCalibur, BD). To quantify the modification efficiency of CP05, tissue-targeting peptides, and PMOs on exosomes, rhodamine-labeled peptides (20 μg) or Lissamine-labeled PMOs (20 μg) were incubated with DiR-labeled exosomes (5 μg) at 4°C for 6 hours and washed with PBS for five times in 2-ml ultracentrifuge tubes, followed by filtration with diafiltration tubes (Millipore) to remove unbound peptides or PMOs before flow cytometry. For dual modification of exosomes, FITC-labeled NP41-CP05 (30 μg) and rhodamine-labeled M12 (30 μg) peptides were incubated with 30 μg of exosomes at 4°C for 6 hours individually or together and washed with PBS and filtered to remove unbound peptides before flow cytometry, as described above.

Coimmunoprecipitation

Cell or exosome pellets were lysed with RIPA lysis buffer (Sangon Biotech) containing protease inhibitor cocktails (Roche). Cell or exosome lysates were spun at 14,000*g* for 30 min, followed by 50,000*g* for 30 min, and the protein concentration was measured with Bradford assay (Sigma-Aldrich). For the coimmunoprecipitation of cell lysates, to avoid the nonspecific binding with beads, total protein (1 mg) was preincubated with 150 μg of protein A–Sepharose

beads (Sigma-Aldrich) for 15 min at 4°C, followed by centrifugation at 1500*g* for 15 min, and the supernatant was recovered. Polyclonal rabbit anti-CD63 or control anti-IgG antibody (1 μg) was co-incubated with protein A–Sepharose beads (150 μg) and the supernatant overnight at 4°C. Subsequently, the beads were washed three times with lysis buffer and harvested, followed by incubation with His-tagged peptides for 2 hours. To remove free peptides, the beads were washed with PBS with Tween 20 for three times. The disassociated complex (20 μl) was used for Western blot with His-tag and/or CD63 antibodies (Santa Cruz Biotechnology) at a dilution of 1:1000. For exosome immunoprecipitation, nickel Dynabeads (Solarbio) were preincubated with 100 μg of His-tagged CP05, CP07, or scrambled CP05 for 2 hours at 4°C. After incubation, beads were washed with washing buffer [20 mM Na_2HPO_4, 500 mM NaCl, and 75 mM imidazole (pH 7.4)] for three times to remove unbound peptides. Recovered beads were incubated with 200 μg of exosome lysates for 30 min at 4°C. After incubation, the supernatant was discarded, beads were washed three times with washing buffer, and exosome lysates were eluted with elution buffer [20 mM Na_2HPO_4, 500 mM NaCl, and 500 mM imidazole (pH 7.4)]. The disassociated complex (20 μl) was used for Western blot with polyclonal rabbit CD63 (1:200; Santa Cruz Biotechnology), Alix (1:1000; Abcam), CD9 (1:1000; Abcam), and CD81 (1:200; Santa Cruz Biotechnology) antibodies and mouse monoclonal Tsg101 (1:200; Santa Cruz Biotechnology) antibodies.

Fluorescence resonance energy transfer assay

FRET assay was used to examine the simultaneous binding of two different peptides on the same exosome. FITC-labeled NP41 (10 μg) (Ex, 488 nm; Em, 520 nm) and rhodamine-labeled RVG (10 μg) (Ex, 525 nm; Em, 625 nm) were incubated with exosomes (10 μg) individually or together and washed with PBS for three times before measurement with a plate reader (EnSpire Multimode Plate Reader, PerkinElmer).

Serum stability assay

CP05 peptides (1 mM) were incubated in PBS containing 20% mouse serum at 37°C. Aliquots of 20 μl were taken at 0, 15, 30, 60, 120, and 360 min and diluted with 10 μl of 10% trichloroacetic acid to precipitate serum protein. The samples were mixed and kept at −20°C for 30 min to allow for complete precipitation. The precipitated serum proteins were removed by centrifugation (13,000 rpm, 5 min), and the supernatant was analyzed by LC-MS.

Tissue distribution

To examine the biodistribution of CP05-modified and homing moiety–CP05–modified exosomes in immunodeficient nude mice and wild-type C57BL/6 mice, DiR-labeled exosomes and AF680-labeled peptides were used. Briefly, exosomes (EXO), CP05-modified exosomes (EXO_{CP05}), and M12-CP05–painted exosomes (EXO_{M12}), RVG-CP05–painted exosomes (EXO_{RVG}), and SP94-CP05–painted exosomes (EXO_{SP94}) (30 μg) were administered intravenously into immunodeficient nude mice, C57BL/6 mice, or mice bearing subcutaneous HCC for a single injection, respectively. For human serum–derived exosomes, Pkh67-labeled exosomes (30 μg) were used for animal imaging studies. Perfusion was performed 2 hours after injection with 50 ml of cold PBS to wash out exosomes in circulation. Body-wide muscles, liver, tumor, kidney, and spleen were harvested for imaging with IVIS spectrum (PerkinElmer).

RNA extraction and nested RT-PCR analysis

Sections were cut, collected, and homogenized in TRIzol reagent (Invitrogen). Total RNA was then extracted, and 200 ng of RNA template was used for a RT-PCR with a OneStep RT-PCR kit (Qiagen). The primer sequences for the initial RT-PCR were 5′-CAGAATTCTGCCAATTGCTGAG-3′ (exon 20 F0) and 5′-TTCTTCAGCTTTTGTGTCATCC-3′ (exon 26 R0) for reverse transcription from mRNA and amplification of complementary DNA from exons 20 to 26. The cycling conditions were 95°C for 1 min, 55°C for 1 min, and 72°C for 2 min for 25 cycles. The primer sequences for the second rounds were 5′-CCCAGTCTACCACCCTATCAGAGC-3′ (exon 20 F1) and 5′-CCTGCCTTTAAGGCTTCCTT-3′ (exon 24 R1). The cycling conditions were 95°C for 1 min, 57°C for 1 min, and 72°C for 1 min for 25 cycles. Products were examined by electrophoresis on a 2% agarose gel. RNA extracted from tibialis anterior muscles of C57BL/6 and mdx mice was used as normal and positive controls. The quantification of full-length and skipped RT-PCR bands is based on densitometry of gel images and analyzed with ImageJ software (https://imagej.nih.gov/ij/).

Protein extraction and Western blot

Exosome pellets were lysed with lysis buffer and subjected to 10% SDS–polyacrylamide gel electrophoresis gels and transferred to a polyvinylidene difluoride membrane. Polyclonal rabbit anti-Alix (1:200; Santa Cruz Biotechnology), anti-CD63 (1:200; Santa Cruz Biotechnology), and anti-CD9 (1:1000; Abcam) antibodies and mouse monoclonal Tsg101 (1:200; Santa Cruz Biotechnology) were used as primary antibodies to confirm the presence of exosomes. Cytochrome c (1:1000; Santa Cruz Biotechnology) was used as the primary antibody to examine the possible contamination of organelles. For dystrophin expression, protein extraction and Western blot were carried out as previously described (*35*). Various amounts of protein from wild-type C57BL/6 mice were used as positive controls, and corresponding amounts of protein from muscles of treated or untreated mdx mice were loaded onto SDS–polyacrylamide gel electrophoresis gels (4% stacking and 6% resolving). The membrane was then washed and blocked with 5% skimmed milk and probed overnight with DYS1 (mouse monoclonal; 1:200; Abcam) for the detection of dystrophin protein and α-actinin (mouse monoclonal; 1:5000; Sigma-Aldrich) as a loading control. The bound primary antibody was detected by peroxidase-conjugated goat anti-mouse IgG (Sigma-Aldrich) and the ECL Western blot analysis system (Millipore). The intensity of the bands obtained from treated mdx muscles was measured by ImageJ software. The dystrophin/α-actinin ratios of treated samples were normalized to the average C57BL/6 dystrophin/α-actinin ratios (from serial dilutions). Each experiment was performed at least three times (at least three animals).

Immunohistochemistry and histology

Sections of 8 μm were cut from tibialis anterior, quadriceps, gastrocnemius, triceps, abdominal and diaphragm, and cardiac muscles. Sections were then examined for dystrophin expression with a rabbit polyclonal antibody 2166 against the dystrophin C-terminal region (the antibody was provided by K. Davies, Department of Physiology, Anatomy and Genetics, University of Oxford). Polyclonal antibodies were detected by goat anti-rabbit IgG Alexa Fluor 594 (Invitrogen). For the colocalization study, sections were examined with a confocal fluorescence microscope (FV1000, Olympus). The serial sections were also stained with a panel of polyclonal and

monoclonal antibodies for the detection of DAPC components. Rabbit polyclonal antibody to neuronal nitric oxide synthase (1:50) and mouse monoclonal antibodies to β-dystroglycan and α-sarcoglycan were used according to the manufacturer's instructions (1:200; Novocastra). The M.O.M. blocking kit (Vector Laboratories) was applied for the immunostaining of the DAPC. To examine the presence of CD3 T lymphocytes and macrophages in tissues from treated mdx mice or controls, mouse tissues were fixed in Bouin's solution (Sigma-Aldrich) and embedded with paraffin. $CD3^+$ T lymphocytes or $CD68^+$ macrophages were stained with rabbit–anti-mouse polyclonal antibodies CD3 (1:200; Abcam) or CD68 (1:500; Abcam) and detected by goat–anti-rabbit secondary antibody. Routine H&E staining was used to examine the overall liver and kidney morphology and assess the level of infiltrating mononuclear cells.

Serum enzyme measurements

Mouse blood was taken immediately after cervical dislocation and centrifuged at 1500 rpm for 3 min. Serum was separated and stored at −80°C. Analysis of levels of serum CK, AST, ALT, ALP, BUN, and Crea was performed by the clinical laboratory (Tianjin Metabolic Disease Hospital, Tianjin Medical University, Tianjin, China).

Functional grip strength

Treated and control mice were tested using a commercial grip strength monitor (Chatillon). Briefly, each mouse was held 2 cm from the base of the tail, allowed to grip a protruding metal triangle bar attached to the apparatus with their forepaws, and pulled gently until they released their grip. The force exerted was recorded, and five sequential tests were carried out for each mouse, averaged at 30 s apart. Subsequently, the readings for force recovery were normalized by the body weight.

Statistical analysis

All data are means ± SEM. Statistical differences between treatment and control groups were evaluated by SigmaStat (Systat Software). Both parametric and nonparametric analyses were applied, in which the Mann-Whitney rank sum test (Mann-Whitney *U* test) was used for samples on a non-normal distribution, whereas a two-tailed *t* test was performed for samples with a normal distribution, respectively.

SUPPLEMENTARY MATERIALS

www.sciencetranslationalmedicine.org/cgi/content/full/10/444/eaat0195/DC1

Fig. S1. In vitro biopanning for exosomal anchor peptides.

Fig. S2. Characterization of myotube-derived exosomes and coimmunoprecipitation assay for verifying the specific binding of CP05 to CD63.

Fig. S3. Validation of flow cytometry assay for exosome measurement and quantitative analysis of CD63 protein on exosomal surface.

Fig. S4. Characterization of M12-CP05–modified exosomes (EXO_{M12}) and exosomes derived from Hepa1-6, human cells, and serum.

Fig S5. Characterization of CP05-PMO–modified exosomes (EXO_{PMO}) and colocalization of DiR-labeled exosomes with dystrophin-positive fibers.

Fig S6. Comparison between single and triple intravenous injection of EXO_{PMO} at the dose of 12.5 mg PMO/kg per week in mdx mice.

Table S1. Nomenclature and sequences of peptides and PMO used in the study.

REFERENCES AND NOTES

1. S. Stremersch, S. C. De Smedt, K. Raemdonck, Therapeutic and diagnostic applications of extracellular vesicles. *J. Control. Release* **244**, 167–183 (2016).
2. K. W. Witwer, E. I. Buzás, L. T. Bemis, A. Bora, C. Lässer, J. Lötvall, E. N. Nolte-'t Hoen, M. G. Piper, S. Sivaraman, J. Skog, C. Théry, M. H. Wauben, F. Hochberg, Standardization of sample collection, isolation and analysis methods in extracellular vesicle research. *J. Extracell. Vesicles* **2**, 20360 (2013).
3. L. A. Burnett, R. A. Nowak, Exosomes mediate embryo and maternal interactions at implantation and during pregnancy. *Front. Biosci. (Schol. Ed.)* **8**, 79–96 (2016).
4. T. L. Whiteside, Tumor-derived exosomes and their role in cancer progression. *Adv. Clin. Chem.* **74**, 103–141 (2016).
5. M. S. Kim, M. J. Haney, Y. Zhao, V. Mahajan, I. Deygen, N. L. Klyachko, E. Inskoe, A. Piroyan, M. Sokolsky, O. Okolie, S. D. Hingtgen, A. V. Kabanov, E. V. Batrakova, Development of exosome-encapsulated paclitaxel to overcome MDR in cancer cells. *Nanomedicine* **12**, 655–664 (2016).
6. Y. Tian, S. Li, J. Song, T. Ji, M. Zhu, G. J. Anderson, J. Wei, G. Nie, A doxorubicin delivery platform using engineered natural membrane vesicle exosomes for targeted tumor therapy. *Biomaterials* **35**, 2383–2390 (2014).
7. L. Alvarez-Erviti, Y. Seow, H. Yin, C. Betts, S. Lakhal, M. J. Wood, Delivery of siRNA to the mouse brain by systemic injection of targeted exosomes. *Nat. Biotechnol.* **29**, 341–345 (2011).
8. M. C. Didiot, L. M. Hall, A. H. Coles, R. A. Haraszti, B. M. Godinho, K. Chase, E. Sapp, S. Ly, J. F. Alterman, M. R. Hassler, D. Echeverria, L. Raj, D. V. Morrissey, M. DiFiglia, N. Aronin, A. Khvorova, Exosome-mediated delivery of hydrophobically modified siRNA for Huntingtin mRNA silencing. *Mol. Ther.* **24**, 1836–1847 (2016).
9. T. Smyth, K. Petrova, N. M. Payton, I. Persaud, J. S. Redzic, M. W. Graner, P. Smith-Jones, T. J. Anchordoquy, Surface functionalization of exosomes using click chemistry. *Bioconjug. Chem.* **25**, 1777–1784 (2014).
10. H. Qi, C. Liu, L. Long, Y. Ren, S. Zhang, X. Chang, X. Qian, H. Jia, J. Zhao, J. Sun, X. Hou, X. Yuan, C. Kang, Blood exosomes endowed with magnetic and targeting properties for cancer therapy. *ACS Nano* **10**, 3323–3333 (2016).
11. E. V. Batrakova, M. S. Kim, Using exosomes, naturally-equipped nanocarriers, for drug delivery. *J. Control. Release* **219**, 396–405 (2015).
12. K. B. Johnsen, J. M. Gudbergsson, M. N. Skov, L. Pilgaard, T. Moos, M. Duroux, A comprehensive overview of exosomes as drug delivery vehicles — Endogenous nanocarriers for targeted cancer therapy. *Biochim. Biophys. Acta* **1846**, 75–87 (2014).
13. S. A. Kooijmans, S. Stremersch, K. Braeckmans, S. C. de Smedt, A. Hendrix, M. J. Wood, R. M. Schiffelers, K. Raemdonck, P. Vader, Electroporation-induced siRNA precipitation obscures the efficiency of siRNA loading into extracellular vesicles. *J. Control. Release* **172**, 229–238 (2013).
14. Z. Andreu, M. Yáñez-Mó, Tetraspanins in extracellular vesicle formation and function. *Front. Immunol.* **5**, 442 (2014).
15. Q. L. Lu, S. Cirak, T. Partridge, What can we learn from clinical trials of exon skipping for DMD? *Mol. Ther. Nucleic Acids* **3**, e152 (2014).
16. S. Fletcher, K. Honeyman, A. M. Fall, P. L. Harding, R. D. Johnsen, J. P. Steinhaus, H. M. Moulton, P. L. Iversen, S. D. Wilton, Morpholino oligomer-mediated exon skipping averts the onset of dystrophic pathology in the mdx mouse. *Mol. Ther.* **15**, 1587–1592 (2007).
17. T. Serizawa, P. Techawanitchai, H. Matsuno, Isolation of peptides that can recognize syndiotactic polystyrene. *Chembiochem* **8**, 989–993 (2007).
18. T. Shtatland, D. Guettler, M. Kossodo, M. Pivovarov, R. Weissleder, PepBank - A database of peptides based on sequence text mining and public peptide data sources. *BMC Bioinformatics* **8**, 280 (2007).
19. J. Huang, B. Ru, S. Li, H. Lin, F. B. Guo, SAROTUP: Scanner and reporter of target-unrelated peptides. *J. Biomed. Biotechnol.* **2010**, 101932 (2010).
20. M. F. Baietti, Z. Zhang, E. Mortier, A. Melchior, G. Degeest, A. Geeraerts, Y. Ivarsson, F. Depoortere, C. Coomans, E. Vermeiren, P. Zimmermann, G. David, Syndecan-syntenin-ALIX regulates the biogenesis of exosomes. *Nat. Cell Biol.* **14**, 677–685 (2012).
21. E. J. van der Vlist, E. N. Nolte-'t Hoen, W. Stoorvogel, G. J. A. Arkesteijn, M. H. Wauben, Fluorescent labeling of nano-sized vesicles released by cells and subsequent quantitative and qualitative analysis by high-resolution flow cytometry. *Nat. Protoc.* **7**, 1311–1326 (2012).
22. X. Gao, J. Zhao, G. Han, Y. Zhang, X. Dong, L. Cao, Q. Wang, H. M. Moulton, H. Yin, Effective dystrophin restoration by a novel muscle-homing peptide–morpholino conjugate in dystrophin-deficient *mdx* mice. *Mol. Ther.* **22**, 1333–1341 (2014).
23. A. Lo, C. T. Lin, H. C. Wu, Hepatocellular carcinoma cell-specific peptide ligand for targeted drug delivery. *Mol. Cancer Ther.* **7**, 579–589 (2008).
24. Z. Lu, B. Zuo, R. Jing, X. Gao, Q. Rao, Z. Liu, H. Qi, H. Guo, H. Yin, Dendritic cell-derived exosomes elicit tumor regression in autochthonous hepatocellular carcinoma mouse models. *J. Hepatol.* **67**, 739–748 (2017).
25. S. Kamerkar, V. S. LeBleu, H. Sugimoto, S. Yang, C. F. Ruivo, S. A. Melo, J. J. Lee, R. Kalluri, Exosomes facilitate therapeutic targeting of oncogenic KRAS in pancreatic cancer. *Nature* **546**, 498–503 (2017).
26. Z. Stickney, J. Losacco, S. McDevitt, Z. Zhang, B. Lu, Development of exosome surface display technology in living human cells. *Biochem. Biophys. Res. Commun.* **472**, 53–59 (2016).
27. M. A. Whitney, J. L. Crisp, L. T. Nguyen, B. Friedman, L. A. Gross, P. Steinbach, R. Y. Tsien, Q. T. Nguyen, Fluorescent peptides highlight peripheral nerves during surgery in mice. *Nat. Biotechnol.* **29**, 352–356 (2011).

28. K. J. Nowak, K. E. Davies, Duchenne muscular dystrophy and dystrophin: Pathogenesis and opportunities for treatment. *EMBO Rep.* **5**, 872–876 (2004).
29. M. Zatz, D. Rapaport, M. Vainzof, M. R. Passos-Bueno, E. R. Bortolini, C. Pavanello Rde, C. A. Peres, Serum creatine-kinase (CK) and pyruvate-kinase (PK) activities in Duchenne (DMD) as compared with Becker (BMD) muscular dystrophy. *J. Neurol. Sci.* **102**, 190–196 (1991).
30. R. van der Meel, M. H. Fens, P. Vader, W. W. van Solinge, O. Eniola-Adefeso, R. M. Schiffelers, Extracellular vesicles as drug delivery systems: Lessons from the liposome field. *J. Control. Release* **195**, 72–85 (2014).
31. E. R. Abels, X. O. Breakefield, Introduction to extracellular vesicles: Biogenesis, RNA cargo selection, content, release, and uptake. *Cell. Mol. Neurobiol.* **36**, 301–312 (2016).
32. P. Ferri, E. Barbieri, S. Burattini, M. Guescini, A. D'Emilio, L. Biagiotti, P. Del Grande, A. De Luca, V. Stocchi, E. Falcieri, Expression and subcellular localization of myogenic regulatory factors during the differentiation of skeletal muscle C2C12 myoblasts. *J. Cell. Biochem.* **108**, 1302–1317 (2009).
33. G.-A. Bounda, W. Zhou, D.-d. Wang, F. Yu, Rhein elicits in vitro cytotoxicity in primary human liver HL-7702 cells by inducing apoptosis through mitochondria-mediated pathway. *Evid. Based Complement. Alternat. Med.* **2015**, 329831 (2015).
34. G. D. Ivanova, A. Arzumanov, R. Abes, H. Yin, M. J. A. Wood, B. Lebleu, M. J. Gait, Improved cell-penetrating peptide-PNA conjugates for splicing redirection in HeLa cells and exon skipping in mdx mouse muscle. *Nucleic Acids Res.* **36**, 6418–6428 (2008).
35. G. Han, B. Gu, L. Cao, X. Gao, Q. Wang, Y. Seow, N. Zhang, M. J. Wood, H. Yin, Hexose enhances oligonucleotide delivery and exon skipping in dystrophin-deficient mdx mice. *Nat. Commun.* **7**, 10981 (2016).

Acknowledgments: We acknowledge W. Niu (Tianjin Metabolic Disease Hospital, Tianjin Medical University, Tianjin, China) and T. Sun (Tianjin Medical University, Tianjin, China) for the assistance with the clinical biochemistry assays and tissue imaging. **Funding:** This study was supported by the National Key R&D Program of China (grant no. 2017YFC1001902), the National Natural Science Foundation of China (grant nos. 81671528, 81672124, 81361128013, 81301526, and 81273420), Tianjin Municipal Science and Technology Key Project (grant nos. 14JCZDJC36000 and 14JCQNJC11000), and Tianjin Municipal 13th 5-year plan (Tianjin Medical University Talent Project). **Author contributions:** Study design: X.G. and H.Y.; laboratory work: X.G., N.R., X.D., B.Z., and Y. S.; blood collection: X.G. and B.Z.; peptide labeling: R.Y. and Q.Z.; peptide conjugation: H.M.M.; data analysis: X.G. and H.Y.; study write-up: H.Y. with the input from all authors. **Competing interests:** H.Y., X.G., B.Z., N.R., and X.D. are inventors on patent application no. 201510520565.7 submitted by Tianjin Medical University that covers anchor peptide CP05 and its conjugates. All other authors declare that they have no competing interests. **Data and materials availability:** All data needed to evaluate the conclusions in the paper are present in the paper and the Supplementary Materials. Additional information related to this paper may be requested from the authors.

Submitted 26 May 2017
Resubmitted 16 January 2018
Accepted 13 March 2018
Published 6 June 2018
10.1126/scitranslmed.aat0195

Citation: X. Gao, N. Ran, X. Dong, B. Zuo, R. Yang, Q. Zhou, H. M. Moulton, Y. Seow, H. Yin, Anchor peptide captures, targets, and loads exosomes of diverse origins for diagnostics and therapy. *Sci. Transl. Med.* **10**, eaat0195 (2018).

Science Translational Medicine

Anchor peptide captures, targets, and loads exosomes of diverse origins for diagnostics and therapy

Xianjun Gao, Ning Ran, Xue Dong, Bingfeng Zuo, Rong Yang, Qibing Zhou, Hong M. Moulton, Yiqi Seow and HaiFang Yin

Sci Transl Med **10**, eaat0195.
First published 6 June 2018
DOI: 10.1126/scitranslmed.aat0195

Target acquired, anchors aweigh

Small cell-derived, membrane-bound extracellular vesicles (exosomes) can be used therapeutically to deliver drugs or modify gene expression, but when given systemically it is difficult to target their distribution. Gao *et al*. developed a peptide, CP05, that binds to CD63, a protein expressed on exosomes. Painting exosomes with CP05 conjugated to a muscle-targeting peptide increased delivery of a splice-correcting oligomer to muscle, which increased dystrophin expression and muscle function in a mouse model of muscular dystrophy. CP05 could also isolate exosomes from human serum. This study demonstrates that CP05 can be used to capture and modify exosomes and their cargo for targeted delivery.